PHYSICAL REVIEW A **90**, 010501(R) (2014)

Relativistic equation-of-motion coupled-cluster method for the double-ionization potentials of closed-shell atoms

Himadri Pathak,[1,*] Aryya Ghosh,[1] B. K. Sahoo,[2] B. P. Das,[3] Nayana Vaval,[1] and Sourav Pal[1]

[1]*Electronic Structure Theory Group, Physical Chemistry Division, CSIR-National Chemical Laboratory, Pune 411008, India*

[2]*Theoretical Physics Division, Physical Research Laboratory, Ahmedabad 380009, India*

[3]*Theoretical Physics and Astrophysics Group, Indian Institute of Astrophysics, Bangalore 560034, India*

(Received 30 April 2014; published 8 July 2014)

We report the implementation of the relativistic equation-of-motion coupled-cluster method to calculate the double-ionization spectra (DI-EOMCC) of the closed-shell atomic systems. This method is employed to calculate the principal valence double-ionization potential values of He and alkaline-earth-metal (Be, Mg, Ca, Sr, and Ba) atoms. Our results are compared with the results available from the NIST database and other *ab initio* calculations. We have achieved an accuracy of $\sim 0.1\%$, which is an improvement over the first-principles T-matrix calculations [Y. Noguchi *et al.*, J. Chem. Phys. **123**, 144112 (2005)]. We also present results using the second-order many-body perturbation theory and the random-phase approximation in the equation-of-motion framework, and these results are compared with the DI-EOMCC results.

DOI: 10.1103/PhysRevA.90.010501 PACS number(s): 31.15.ac, 31.15.bw, 32.10.Hq

Recent advances in experimental techniques, such as the x-ray free-electron laser of Linac Coherent Light sources of SLAC [1,2] and attosecond pulses [3,4], have enabled studies of multi-ionization processes. The double photoionization of atoms in which two electrons are ejected to continuum orbitals is a three-body quantal problem. The complex interplay between the relativistic effects and the electron correlation is of central importance in the accurate description of these processes [5]. The generation of attosecond pulses is an important milestone in the development of ultrafast laser spectroscopy. It can be used to study the dynamics of correlated electrons in double ionization processes in atoms and molecules [6,7]. One of the outstanding theoretical problems in these studies is to explain the simultaneous double-ionization mechanisms [8], which are different than the sequential ionization events. There has been experimental progress in the direction of attosecond tracing of the correlated electron emissions in the nonsequential double-ionization processes in atomic systems which requires a suitable theory that could describe the effects of the dynamical electron corrections adequately [9]. To complement the sophisticated experimental techniques, it is desirable to have accurate theoretical methods to treat the double-ionization continua. Attempts have been made using the T-matrix [10,11], Δ self-consistent-field [12], and the four-component two-particle propagator methods [13,14]. It is well known that not only the electron correlation, but also the relaxation effects play a significant role in the accurate description of atomic states. Therefore measurements and calculations based on the lower-order many-body methods do not agree with each other [15]. The equation-of-motion coupled-cluster (EOMCC) method [16–18] provides a balanced treatment of the electron correlation and relaxation effects to determine the atomic states and to also calculate differences of the energies in a direct manner. It uses a large configurational space constructed from the occupied and virtual spinors that takes into account both the static and dynamic correlations simultaneously. The wave functions and energies of all the states of interest are obtained through the diagonalization of a similarity-transformed Hamiltonian, which in a sense is associated with the multireference theory, but the EOMCC is operationally single reference in nature. The (0,1) sector Fock space multireference (FSMRCC) [19,20] theory is equivalent to the EOMCC method for the single-ionization problem [21], but this is not the case for the (0,2) sector FSMRCC and the double-ionization EOMCC (DI-EOMCC) methods. The FSMRCC theory uses the amplitude equations of all the lower sectors along with the amplitudes of that particular sector, whereas EOMCC requires the amplitudes of the sector of interest and those of the (0,0) sector.

The electronically excited molecules or atoms relax through various radiationless mechanisms by emitting electrons. The precise values of the ionization potentials (IPs) and double-ionization potentials (DIPs) are important to analyze these relaxation processes and to understand the excited states of the emitter [22]. Furthermore, these processes play significant roles in designing efficient radio oncology schemes, which can be used as powerful tools to investigate the genotoxic effects on living tissues [23]. Bartlett and co-workers were the first to implement the EOMCC method to calculate DIPs [24]; however, their work was in the nonrelativistic regime. Recently, we have implemented the relativistic EOMCC method and used it to calculate IPs of various atomic systems [25]. In this work, we extend the idea of single electron ionization using the relativistic EOMCC method to the domain of the double-ionization spectra by considering simultaneous removal of two electrons from the closed-shell atomic systems.

Development of the relativistic DI-EOMCC method is a step forward as it can be used for studying various photoionization spectra, highly energetic electron scattering processes, and various electronic decay processes, especially the Auger spectra in the atomic systems. The alkaline-earth-metal atoms are well suited for studying the double-ionization spectra, as the outer valence electrons are well separated from the rest of the electrons. The He atom is also similar to these atoms, though they have different radial structures of the ns

*h.pathak@ncl.res.in

orbitals. As a first application of our relativistic DI-EOMCC method, we have calculated the valence DIPs of He, Be, Mg, Ca, Sr, and Ba atoms. The computed results are compared with the values from the NIST database [26] and with the available calculations based on the first-principles T-matrix approach [11]. We would also like to mention that, though we have calculated valence DIPs of the closed-shell atoms, the implemented DI-EOMCC method is applicable to both closed-shell and open-shell atomic and molecular systems having any number of valence electrons.

We also present results using two intermediate schemes at the second-order many-body perturbation theory [MBPT(2)] and the random-phase approximation (RPA) level in the EOMCC framework to assess the roles of the electron correlation effects. The former uses first-order perturbed wave function, which corresponds to MBPT(2) energy as the ground state energy. For the latter, the effective Hamiltonian matrix elements are constructed only in the two hole ($2h$) space. It is clear that in both these approaches, the electron correlation effects are not treated as comprehensively as they are in the four-component all-electron DI-EOMCC approach.

The starting point for the EOMCC method is the single reference CC wave function $|\Psi_0\rangle$, which is of the form

$$|\Psi_0\rangle = e^{\hat{T}_n}|\Phi_0\rangle, \tag{1}$$

where $|\Phi_0\rangle$ is the Dirac-Hartree-Fock (DF) reference determinant and the cluster operators are of the form

$$\hat{T}_n = \sum_{\substack{a_1<a_2\cdots<a_n \\ i_1<i_2\cdots<i_n}}^{M} t_{i_1 i_2\cdots i_n}^{a_1 a_2\cdots a_n}\, a_1^\dagger i_1 a_2^\dagger i_2 \cdots a_n^\dagger i_n, \tag{2}$$

where $i,\ldots$ $(a,\ldots)$ corresponds to the strings of creation and annihilation operators acting on the reference determinant of M numbers of occupied electrons and stands for the hole and particle indices, respectively. Projection onto the excited determinants $|\Phi_{i_1 i_2\cdots i_n}^{a_1 a_2\cdots a_n}\rangle = a_1^\dagger i_1 a_2^\dagger i_2 \cdots a_n^\dagger i_n|\Phi_0\rangle$, we get the simultaneous nonlinear algebraic equations for the correlation energy, defined as $\Delta E_{\rm corr} = E_g - E_{\rm DF}$ for the ground state energy E_g of the state $|\Psi_0\rangle$ and DF energy $E_{\rm DF}$ of the state $|\Phi_0\rangle$, and also for the unknown cluster amplitudes of any order of excitations

$$\left\langle \Phi_{i_1 i_2\cdots i_n}^{a_1 a_2\cdots a_n}\right|(\hat{H}_N e^{\hat{T}})_c|\Phi_0\rangle = \Delta E_{\rm corr}\delta_{n,0} \quad (n=0,\ldots,k). \tag{3}$$

In the above equation, subscript c means connected, n is the level of excitations from the DF state, and $\hat{H}_N = \hat{H} - \langle\Phi_0|\hat{H}|\Phi_0\rangle$ is the normal ordered form of the Dirac-Coulomb Hamiltonian ($\hat{H}$) which is given by

$$\hat{H} = \sum_i \left[c\boldsymbol{\alpha}_i\cdot\mathbf{p}_i + (\beta_i - 1)c^2 + V_{\rm nuc}(r_i) + \sum_{j>i}\frac{1}{r_{ij}}\right], \tag{4}$$

where $\boldsymbol{\alpha}_i$ and β_i are the usual Dirac matrices, $V_{\rm nuc}(r_i)$ is the nuclear potential, and $\frac{1}{r_{ij}}$ is the electron-electron repulsion potential. The single particle energies are evaluated with respect to the rest mass energy ($-c^2$) of the electron. Note that unless stated otherwise, we use atomic units (a.u.) in this Rapid Communication. In our calculations, we only consider single and double excitations ($n=2$), which is referred to as the CCSD method.

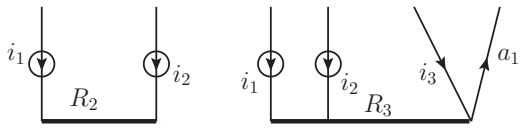

FIG. 1. Diagrammatic form of the R_2 and R_3 operators. Lines with down and up arrows denote the occupied and unoccupied orbitals, respectively. An arrow with a circle means a detached occupied orbital.

In the DI-EOMCC approach, the wave function for the μth state of the doubly ionized system ($M-2$ electron) can be written as

$$|\Psi_\mu\rangle = R_\mu^{M-2}|\Psi_0\rangle, \quad \mu = 1,2,\ldots. \tag{5}$$

The R_μ^{M-2} is a linear operator and it is of the form

$$\begin{aligned} R_\mu^{M-2} &= R_2 + R_3 + \cdots \\ &= \sum_{i_1<i_2} r_{i_1 i_2} i_2 i_1 + \sum_{\substack{a_1 \\ i_1<i_2<i_3}} r_{i_1 i_2 i_3}^{a_1} a_1^\dagger\, i_3 i_2 i_1 + \cdots. \end{aligned} \tag{6}$$

In our approximation, we considered up to the R_2 and R_3 operators which are diagrammatically shown in Fig. 1.

The difference ($\Delta E_\mu = E_\mu - E_g$) between the energies of the ground and the doubly ionized states (E_μ) are calculated

$$\left[\bar{H}_N, \hat{R}_\mu^{M-2}\right]|\Phi_0\rangle = \Delta E_\mu \hat{R}_\mu^{M-2}|\Phi_0\rangle \quad \forall\mu, \tag{7}$$

on projecting onto the basis of excited determinants ($|\phi_{i_1 i_2}\rangle$ and $|\phi_{i_1 i_2 i_3}^{a_1}\rangle$) with respect to $|\phi_0\rangle$, yields the matrix form,

$$\bar{H}_N R = R\Delta E. \tag{8}$$

Here, $\bar{H}_N = (\hat{H}_N e^T)_c$ is the similarity-transformed effective Hamiltonian. In our present implementation of the DI-EOMCC method, the matrix elements of the $\bar{H}_N$ Hamiltonian are constructed in the $2h$ and $3h$-$1p$ space and diagonalized to obtain the desired eigenvectors and eigenvalues. The antisymmetrized diagrams contributing to the $2h$ and $3h$-$1p$ blocks are presented in Figs. 2 and 3, respectively. The diagrams corresponding to the $2h$ block are responsible for the RPA calculations. These diagrams are evaluated with the help of the one-body, two-body, and three-body intermediate diagrams.

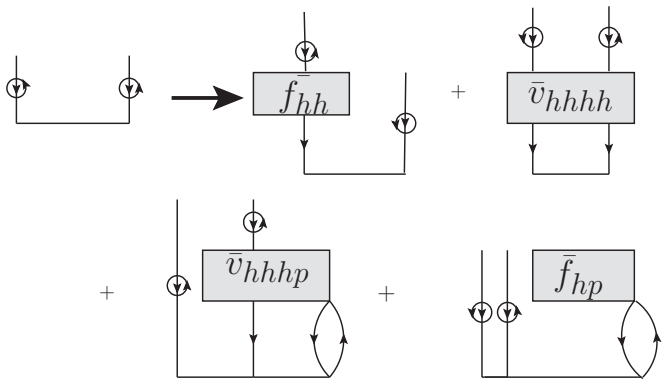

FIG. 2. Diagrams contributing to the $2h$ block.

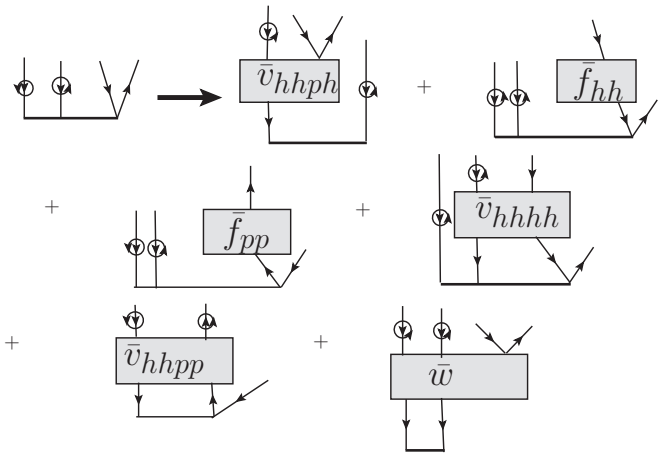

FIG. 3. Diagrams contributing to the $3h$-$1p$ block.

The evaluation of the intermediate diagrams requires the solution of the CCSD equations. The intermediate diagrams are constructed by contracting the one-body and two-body parts of the effective Hamiltonian with the converged T_1 and T_2 amplitudes. The one-body intermediate diagrams are inserted in Figs. 2 and 3 as $\bar{f}_{hh}$, $\bar{f}_{pp}$, and $\bar{f}_{hp}$. There are four distinct types of two-body intermediate diagrams required for the construction of the $\bar{H}_N$ matrix elements for the DI-EOMCC calculations. These are also used as $\bar{v}_{hhhh}$, $\bar{v}_{hhhp}$, $\bar{v}_{hhph}$, and $\bar{v}_{hhpp}$ in the above two figures. The three-body intermediate diagram is also shown in Fig. 3 as $\bar{w}$.

The dimension of the $\bar{H}_N$ matrix is very large ($nh^2 + nh^3np$, $nh^2 + nh^3np$) and it is not amenable to a full diagonalization scheme. Here nh and np denote the number of holes and particles, respectively. We have, therefore, used the Davidson algorithm [27], which is an iterative scheme, to diagonalize the $\bar{H}_N$ matrix. It avoids computation, storage, and diagonalization of the full matrix. The Davidson algorithm performs reasonably well for the whole spectrum, but we have solved only for the root corresponding to the lowest eigenvalue.

The orbital basis sets were generated using the proper kinetic balance between the large and small components of the wave function, where the large component of the wave function is constructed using the linear combinations of the Gaussian-type of orbitals (GTOs) as $g^L_{kp}(r) = C^L_{ki} r^{n_\kappa} e^{-\alpha_p r^2}$, with the imposed condition $\alpha_p = \alpha_0 \beta^{p-1}$, where $p = 0,1,\ldots,k$ with k number of GTOs. The corresponding α_0 and β parameters for all the atoms along with the number of GTOs generated at the DF level are given in Table I. The orbital basis is constructed by taking into account primitive functions up to g harmonics. It is impractical to use of all the orbitals generated in the DF method in a correlation calculation. Therefore, we have considered all the occupied orbitals, and for the virtual orbitals certain threshold energies, since the contributions from the high-lying orbitals is rather small owing to their large energy values. These orbitals are referred to as active orbitals. The two-parameter finite-size Fermi charge density distribution nuclear model $\rho_{\rm nuc}(r) = \frac{\rho_0}{1+e^{(r-b)/a}}$, is used to evaluate the nuclear potential; here ρ_0 is the average nuclear density, b is the half-charge radius, and a is related to the skin thickness.

TABLE II. DF ($E^0_{\rm DF}$) and correlation energies from the MBPT(2) ($\Delta E^{(2)}_{\rm corr}$) and CCSD ($\Delta E^{\rm (CCSD)}_{\rm corr}$) methods along with the number of active orbitals used.

	No. of active orbitals							
Atom	s	p	d	f	g	$E^0_{\rm DF}$	$\Delta E^{(2)}_{\rm corr}$	$\Delta E^{\rm (CCSD)}_{\rm corr}$
He	17	15	13	9	7	−2.8618	−0.0365	−0.0416
Be	14	12	12	10	10	−14.5758	−0.0748	−0.0929
Mg	20	14	12	11	10	−199.9350	−0.4097	−0.4195
Ca	16	15	12	11	10	−679.7100	−0.7515	−0.7648
Sr	16	13	13	12	10	−3178.0797	−1.6530	−1.5922
Ba	16	15	14	12	9	−8135.6428	−2.2556	−2.1258

In Table II, we present the DF energy ($E^0_{\rm DF}$) and the correlation energies from the MBPT(2) ($E^2_{\rm corr}$) and the CCSD ($E^{\rm CCSD}_{\rm corr}$) methods along with the number of active orbitals corresponding to each symmetry used in the calculations. In Table III, we present the results for the valence DIPs of the He, Be, Mg, Ca, Sr, and Ba atoms. In fact, the formulation of the present method is valid even for determining DIPs of the states including inner occupied orbitals; however, they require larger dimensional space and special care on account of the higher-order correlation effects in the considered systems, and are left for a future work. All these results are compared with the tabulated values of the NIST database [26] and with the available results from the first-principles T-matrix calculations [11]. The differences between the DI-EOMCC (given in the table as EOMCC) results and the NIST data are plotted as δ (in percent) in Fig. 4. All the calculated DIPs are in excellent agreement with those of the NIST data. The DI-EOMCC values differ by about 0.01–0.02 eV from the NIST values except for the He atom, where the agreement is even better. It is found that MBPT(2) underestimates the values of the DIPs relative to the DI-EOMCC as the dominant part of the dynamic correlation is missing in this scheme.

TABLE I. The number and the α_0 and β parameters used for the GTOs to generate single particle orbitals at the DF level.

		s		p		d		f		g	
Atom	Number of orbitals	α_0	β	α_0	β	α_0	β	α_0	β	α_0	β
He	(36s,35p,34d,33f,32g)	0.00075	2.075	0.00155	2.080	0.00258	2.180	0.00560	2.300	0.00765	2.450
Be	(36s,35p,34d,33f,32g)	0.00500	2.500	0.00615	2.650	0.00505	2.550	0.00500	2.530	0.00480	2.500
Mg	(35s,34p,33d,32f,31g)	0.02950	1.630	0.09750	1.815	0.00750	2.710	0.00780	2.730	0.00800	2.750
Ca	(35s,34p,33d,32f,31g)	0.00895	2.110	0.00815	2.150	0.00750	2.500	0.00700	2.550	0.00690	2.600
Sr	(35s,34p,33d,32f,30g)	0.01850	2.030	0.04750	2.070	0.00910	2.090	0.00950	2.100	0.00950	2.300
Ba	(35s,34p,33d,32f,31g)	0.00925	2.110	0.00975	2.040	0.00995	2.010	0.01015	2.035	0.01035	2.038

TABLE III. Double-ionization energies of the alkaline-earth-metal (Be, Mg, Ca, Sr, and Ba) and He atoms in eV.

	NIST	This work			T matrix
Atom	[26]	MBPT(2)	RPA	EOMCC	[11]
He	79.0051	78.8596	79.0061	79.0092	
Be	27.5338	27.0949	27.5595	27.5421	27.79
Mg	22.6815	22.4369	22.7655	22.6624	22.97
Ca	17.9848	17.9007	18.0893	17.9992	17.82
Sr	16.7251	16.7119	16.8502	16.7370	
Ba	15.2154	15.2950	15.3546	15.2356	

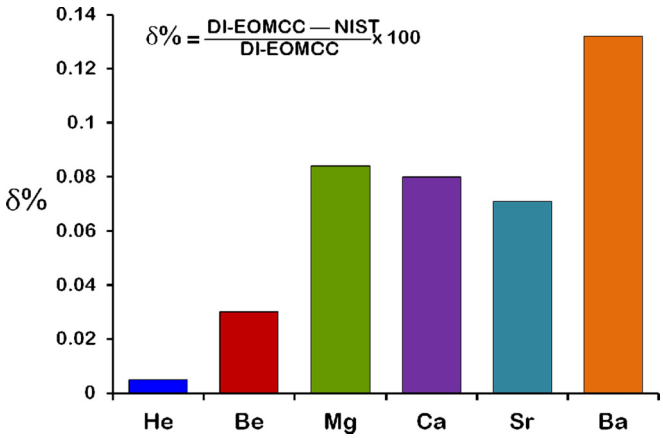

FIG. 4. (Color online) Relative deviations in percent from the NIST values.

RPA, on the other hand, overestimates them except for the He atom. The $3h$-$1p$ block, which is the major source of the nondynamical correlation effects, is missing in the RPA scheme. Our DI-EOMCC results are more accurate than those obtained using the first-principles T-matrix method. The results of the latter differ from the NIST values by about 0.2–0.3 eV.

In conclusion, we have successfully implemented the relativistic EOMCC method to calculate the double-ionization spectra. As a first application, we have calculated the valence DIPs of the alkaline-earth-metal atoms along with the He atom. We have achieved an accuracy of $\sim$0.1%, which is better than all previous DIP calculations. We have also compared the results of our MBPT(2) and RPA calculations with those of DI-EOMCC to highlight the roles of the correlation effects to attain high-precision results.

H.P. and S.P. acknowledge a grant from CSIR XIIth Five Year Plan project on Multi-Scale Simulations of Material (MSM) and the resources of the Center of Excellence in Scientific Computing at CSIR-NCL. B.K.S. acknowledges PRL 3TFlop HPC cluster for the computation.

[1] W. Ackermann *et al.*, Nat. Photon. **1**, 336 (2007).
[2] N. Rohringer *et al.*, Nature (London) **481**, 488 (2012).
[3] G. Sansone *et al.*, Science **314**, 443 (2006).
[4] E. Goulielmakis *et al.*, Science **320**, 1614 (2008).
[5] I. P. Grant, *Relativistic Quantum Theory of Atoms and Molecules: Theory and Computation* (Springer, New York, 2010).
[6] S. Chen, C. Ruiz, and A. Becker, Phys. Rev. A **82**, 033426 (2010).
[7] F. Krausz and M. Ivanov, Rev. Mod. Phys. **81**, 163 (2009).
[8] R. Panfili, Ph.D. thesis, University of Rochester, 2002.
[9] B. Bergues *et al.*, Nat. Commun. **3**, 813 (2012).
[10] M. Springer, F. Aryasetiawan, and K. Karlsson, Phys. Rev. Lett. **80**, 2389 (1998).
[11] Y. Noguchi, Y. Kudo, S. Ishii, and K. Ohno, J. Chem. Phys. **123**, 144112 (2005).
[12] J. Niskanen, P. Norman, H. Aksela, and H. Agren, J. Chem. Phys. **135**, 054310 (2011).
[13] M. Pernpointner, J. Phys. B **43**, 205102 (2010).
[14] M. Pernpointner, J. P. Zobel, and Nikolai V. Kryzhevoi, Phys. Rev. A **85**, 012505 (2012).
[15] M. Seakins, W. J. Griffiths, F. M. Harris, S. R. Andrews, and D. E. Parry, Org. Mass Spectrom. **28**, 1144 (1993).
[16] H. Sekino and R. J. Bartlett, Int. J. Quantum Chem. **26**, 255 (1984).
[17] R. J. Bartlett and J. F. Stanton, in *Reviews in Computational Chemistry*, edited by K. B. Lipkowitz and D. B. Boyd, Vol. 5 (VCH, New York, 1994), p. 65.
[18] J. F. Stanton and R. J. Bartlett, J. Chem. Phys. **98**, 7029 (1993).
[19] R. J. Bartlett and M. Musiał, Rev. Mod. Phys. **79**, 291 (2007).
[20] D. Mukherjee and S. Pal, Adv. Quantum Chem. **20**, 291 (1989).
[21] M. Musiał, S. A. Kucharski, and R. J. Bartlett, J. Chem. Phys. **118**, 1128 (2003).
[22] L. S. Cederbaum, Y-C. Chiang, P. V. Demekhin, and N. Moiseyev, Phys. Rev. Lett. **106**, 123001 (2011).
[23] E. Alizadeh and L. Sanche, Chem. Rev. **112**, 5578 (2012).
[24] M. Musiał, A. Perera, and R. J. Bartlett, J. Chem. Phys. **134**, 114108 (2011).
[25] H. Pathak, B. K. Sahoo, B. P. Das, N. Vaval, and S. Pal, Phys. Rev. A **89**, 042510 (2014).
[26] See http://physics.nist.gov/PhysRefData/ASD/ionEnergy.html
[27] E. R. Davidson, J. Comput. Phys. **17**, 87 (1975).